DYNAMICS OF ELECTRO MAGNETIC FORMATION FLING SATELLITES IN LEO

Shin-ichiro Sakai[1], Ryosuke Kaneda[2], Ken Maeda[3], Tetsu Saitoh[4], Hirobumi Saito[1], Tatsuaki Hashimoto[1]

[1]Institute of Space and Astronautical Science , Japan Aerospace Exploration Agency (ISAS/JAXA), [2]University of Tokyo, [3]NEC Corporation, [4]NEC Aerospace Systems

3-1-1 Yoshinodai, Sagamihara, Kanagawa 229-8510, Japan

sakai@isas.jaxa.jp

Abstract

Electromagnetic formation flight (EMFF) for satellites in LEO is discussed. EMFF is a technique to control the satellites' relative position using electromagnetic force without any propellants. It is estimated that the superconductive magnets have capability to produce required magnetic force for formation keeping. The problem to use EMFF in LEO is the huge amount of disturbance torque, caused by enormous magnetic moment and earth magnetic field. Sinusoidal driving of the superconductive coil is proposed for this issue, and novel method is also proposed for magnetic force control using phase difference between the magnetic moments. Proposed methods are evaluated with experiments with actual superconductive coil, and hardware in the loop simulations is also carried out to demonstrate the relative position control capability of proposed system.

1 Introduction

Formation flight is expected to bring out new possibility of space missions. One important issue of formation flying satellites is the amount of propellants, when conventional propulsion system is applied to keep the formation. It often limits the mission lifetime. Electromagnetic formation flight (EMFF) technique is proposed to keep the formation without any propellants, and overcome this problem [1] [2]. This technique uses electromagnetic force generated by magnetic dipole on each satellite. Usually, huge amount of magnetic dipole is required to keep the formation against Kepler motion, and it requires superconducting coil to be equipped.

To apply such electromagnetic formation flight technique for low earth orbit missions, interference between huge magnetic dipole and earth magnetism causes problems. It generates huge torque on the satellite, and the angular momentum rapidly excess momentum wheel capability. To suppress this interference, polarity of magnetic dipole should changes in short period, compared to the orbital period. The authors also proposed to use inductance-capacitance resonant circuit to change magnetic dipole polarity [3]. Desired electromagnetic force can be generated with proper phase difference between exciting current, and this phase difference can be controlled with impulse voltage input. The advantage of this proposed method is its small energy consumption.

This paper describes the details of this proposed method. Experiments are also curried out and demonstrats the current phase control using actual superconducting coil, and it reveals the effectiveness of our method. It is also demonstrated with hardware in the loop simulation, which combines satellite dynamics model and actual superconducting coil circuit.

2 Formation Control Using Magnetic Force in LEO

2.1 Mission Example and Satellite Configuration

This paper discusses on formation flight missions in LEO. It is known that farther orbit, such as Halo orbit around the second libration point of the Sun-Earth system (L2), is also attractive from the view point of perturbations, thermal environment and so on. However, lower orbit has another advantage such as lower launch cost, higher data rate of communication link, etc. In addition, X-ray or Gamma-ray observation hate radiation belts and prefer LEO. To discuss the control system design in the concrete, here some example LEO mission is assumed. The example mission in this paper is some X-ray or Gamma-ray observation. It means that the mission consists of two satellites, such as mirror and detector. These two satellites are called here "Target" and "Chaser" (Fig. 1). The chaser satellite controls the relative position to maintain the formation, in contrast to the target one which has no ability of active position control. To function as a telescope, the relative position must be maintained in inertial coordinate, to point some target. It is assumed that the focal length or satellite distance should be maintained to be 10[m], with accuracy of 2 [mm]. In this example mission, both satellites weigh 500 [kg] and are injected into LEO of about 600[km] altitude.

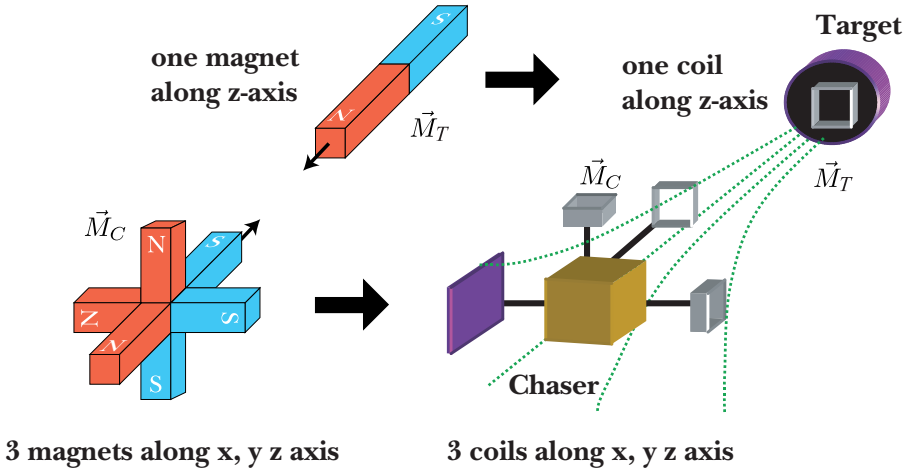

Fig. 1: Formation flight with super-conducting magnets

2.2 Required Force and Magnetic Moment

The required force to maintain the relative position in LEO can be calculated,

$$\rho\omega_k^2 \leq a \leq \rho\omega_k^2\sqrt{1+3\cos^2\theta}, \tag{1}$$

where a and ω_k are the magnitude of control acceleration and orbital angular velocity, respectively [3]. θ is the inclining angle of the relative position vector against the orbital plain. Equation 1 describes the minimum and maximum required force during orbital period. Formation with $\theta = 90$[deg] means the "orbit normal" formation case, depicted in Fig. 2, and the required force is independent from the satellite position in orbit (eq. 1). On the contrary, $\theta = 0$[deg] "in-orbit" separation (Fig 2) requires force varying between $\rho\omega_k$ and $2\rho\omega_k$. Obviously, the latter case is more challenging case from the view point of control, thus "in-orbit" formation ($\theta = 0$[deg]) is discussed in this paper.

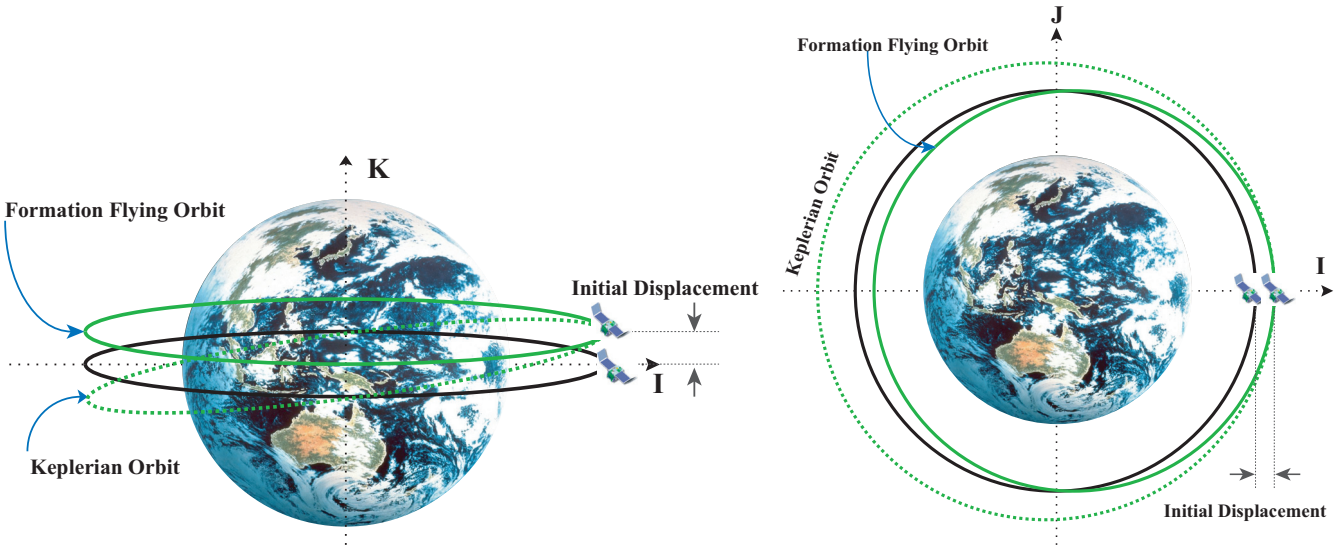

Fig. 2: "Orbit normal"(left) and "In-orbit"(right) formations.

Reference [3] calculates required force in orbital coordinate system, and it can be transformed into inertial coordinate. For "in-orbit" formation case, it is

$$\boldsymbol{F} = \frac{\mu_m \rho \omega_k^2}{2} \begin{bmatrix} -3\sin 2\omega_k t \\ 0 \\ -1 - 3\cos 2\omega_k t \end{bmatrix}. \tag{2}$$

μ_m denotes reduced mass of satellite [1],

$$\mu_t = \frac{m_C m_T}{m_C + m_T}, \tag{3}$$

where m_T, m_C are the mass of target and chaser satellites, respectively. This force is disturbance force to the position control system, thus it is called "orbital disturbance" or "tidal disturbance" in this paper. The frequency of this disturbance force is 2 ω_k, as shown in Eq. 2.

When $\boldsymbol{M_T}$ and $\boldsymbol{M_C}$ denote the magnetic dipole moments on target and chaser satellites respectively, magnetic force acting on the chaser target can be described as follows [2],

$$\boldsymbol{F} = \nabla \left(\boldsymbol{M_C} \cdot \boldsymbol{B_C} \right), \tag{4}$$

where B_C is the magnetic flux density, which can be formulated with $\boldsymbol{M_T}$,

$$\boldsymbol{B_C} = \frac{\mu_0}{4\pi} \left(-\frac{\boldsymbol{M_T}}{\rho^3} + \frac{3(\boldsymbol{M_T} \cdot \boldsymbol{\rho})}{\rho^3} \boldsymbol{\rho} \right) + \boldsymbol{B_{EC}}. \tag{5}$$

where μ_0 is the permeability of free space, $\boldsymbol{B_{EC}}$ is the magnetic flux density caused by the Earth magnetic field, and $\boldsymbol{\rho}$ is the relative position vector between the satellites. For example, if two magnetic moments of the same magnetic moment M align with distance ρ, magnetic force F_{mag} is

$$F_{\text{mag}} = \frac{3\mu_0 M^2}{2\pi r^4}. \tag{6}$$

Equations 1 and 6 suggest the requried amount of magnetic moments. Reference [4] plots this relations versus relative distance. The example mission in this paper assumes the distance

[1] Note that action-reaction force is discussed here.

[2] Note that EB formulation is used here, not EH formulation, thus unit of magnetic moment is [Am^2], not [Wbm]

of 10 [m] and orbit altitude 600 [km], which means $\omega_k = 0.0011$[rad/sec], and Eq. 1 estimates the magnitude of orbital disturbance force to be 6.1 [mN]. Magnetic moments of 30,000 [Am^2] generates 54 [mN] force with Eq. 6, and can overcome the tidal disturbance force, even if the efficiency is down with sinusoidal driving described in the following sections.

2.3 Necessity of Alternating Magnetic Moment

Then the influence of earth magnetic field should be considered. Magnetic force is proportional to the spatial gradient of magnetic field, as Eq. 4 shows, thus the force on the magnetic moment caused by earth magnetic filed is negligible. However, the magnetic torque is proportional to the magnitude of magnetic field,

$$\boldsymbol{T} = \boldsymbol{M} \times \boldsymbol{B}. \tag{7}$$

Roughly speaking, the magnetic moment of 30,000 [Am^2] generates about 0.9 [Nm] DC torque, which is not able to be accumulated in practical momentum wheels.

For this problem, the authors proposed to use alternating magnetic moment [3]. If sinusoidal magnetic moment such as $M = M_0 \sin(\omega_c t)$ is applied, and if the angular frequency ω_c is much higher than the frequency of magnetic field or orbital angular frequency ω_k, then this accumulation of angular momentum comes to be small enough.

To control the magnetic force with such sinusoidal moments, the authors proposed to use the phase difference between the target and chaser magnetic moment [4]. If magnetic moment on chaser satellite has phase difference ϕ compared to the target magnetic moments, simplified example Eq. 6 turns into

$$F_{\mathrm{mag}} = \frac{3\mu_0 M_0^2}{4\pi r^4} \left(\cos(2\omega_c t + \phi) - \cos\phi\right), \tag{8}$$

and the average of F_{mag} during a period is

$$\langle F_{\mathrm{mag}} \rangle = -\frac{3\mu_0 M^2}{4\pi r^4} \cos\phi. \tag{9}$$

Equation 9 indicates that DC components of magnetic force can be changed with the phase difference ϕ, thus it can be used as a control input if the feedback controller bandwidth is much lower than ω_c. In other words, the first term of Eq. 8 behaves as disturbance force around this DC components, with frequency of 2 ω_c. This disturbance is called "coil 2 ω_c disturbance" in the following parts. Note that this frequency is always higher than the control bandwidth, thus it can not be suppressed by relative position control system. From the view points of controller bandwidth or disturbance frequency, coil driving frequency ω_c should be high enough. However, there is some trade-off on frequency choice, since higher frequency results high coil voltage. Relationship between the frequency and disturbance force gives some suggestions about the "optimal" frequency in this trade-off. To evaluate the relative position error caused by 2 ω_c components of magnetic force, transfer function from the disturbance to position error should be considered. Since the frequency ω_c is out of the control bandwidth as mentioned above, it can be calculated only with satellite dynamics of translational motion,

$$P(s) = \frac{1}{\mu s^2}, \tag{10}$$

where s denotes Laplace operator. With this dynamics and AC components of Eq. 8, relative position error can be expressed

$$\epsilon_{\omega_c} = \frac{3\mu_0 M^2}{4\pi\rho^4} \frac{1}{4\omega_c^2 \mu}. \tag{11}$$

As mentioned in 2.1, assumed accuracy requirement is 2 [mm]. Then ω_c is chosen here to be 0.08 [Hz], which causes 0.11[mm] $2\omega_c$ position error as Eq. 11 shows.

2.4 Understanding about the Gravity Gradient Torque on the System

Torque on the magnetic moment caused by earth magnetic field is briefly mentioned in the previous subsection. Here we discuss on magnetic torque which appears in the target-chaser system. Substituting the first term of Eq. 5 into Eq. 7 and simplified using same assumption as Eq. 6, magnetic torque on chaser caused by target's magnetic field, T_{TC}, is

$$T_{TC} = \frac{\mu_0 M_0^2}{4\pi\rho^3} \left(\cos(2\omega_c t + \phi) - \cos\phi\right). \tag{12}$$

In this equation, the average of the first term is equal to zero, however, the second term depends on the phase different ϕ, or the magnetic force to control the formation. This relationship indicates the important aspect of EMFF.

When two satellites are "connected" with magnetic force, then it can be considered as a long rigid rod. Such a long rod in LEO is, of course, affected by gravity gradient torque. Cross product of Eq. 2 and $[0, 0, r]^t$ gives this torque $\boldsymbol{T_{gg}}$,

$$\boldsymbol{T_{gg}} = \left[0, \quad \frac{3}{2}\mu_m \rho^2 \omega_k^2 \sin 2\omega_k t, \quad 0\right]. \tag{13}$$

Time integration of this torque results the angular momentum, L_{gg},

$$\boldsymbol{L_{gg}} = \left[0, \quad -\frac{3}{4}\mu_m \rho^2 \omega_k \cos 2\omega_k t, \quad 0\right], \tag{14}$$

and the amplitude can be calculated to be 20.2 [Nms], using $\mu_m = 250$[kg], ω_k=0.0011 [rad/sec] and ρ=10[m]. Since EMFF maintain the formation with magnetic force, or internal force, this angular momentum of Eq. 14 must be accumulated in the system. Therefore, to maintain the formation in inertial frame, two satellites must accumulate this angular momentum, and to maintain the satellite attitude, the remaining possibility is the momentum wheels on the satellites. In another words, magnetic moment to generate control magnetic force also generates torque in the magnetic field of the other satellite, as shown in Eq. 12. This is an external torque for each satellite, and the wheels on each satellite were driven to cancel this magnetic torque, then finally, the angular momentum is accumulated in the momentum wheels. The authors point out here that this is important understanding about EMFF mechanism. Figure 3 shows the summary of such force and torque affected in two systems: Earth - satellite system and satellite - satellite system. Note that force between the Earth and a satellite, F_{emag}, is negligible. This F_{emag} can be calculated with almost the same equation as Eq. 6,

$$F_{\text{emag}} = \frac{3\mu_0 M M_{\text{earth}}}{2\pi r_{\text{earth}}^4}. \tag{15}$$

where M_{earth} is the magnetic moment of the Earth dipole model (7.9×10^{22}[Am^2]) and r_{earth} is the distance between this Earth dipole moment and the satellite (7000 [km]). If substitute these values into Eq. 15 and compare with the result of Eq. 6, 54[mN], it can be understood that the magnetic force between the Earth and a satellite is about 1.0×10^{-5} times smaller than the magnetic force between two satellites.

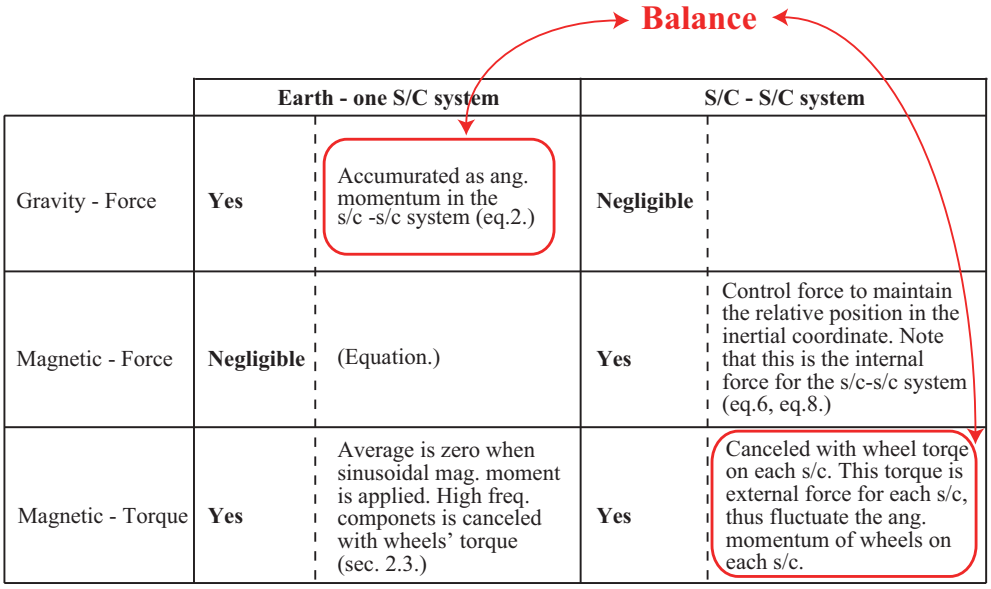

Fig. 3: Balnace of each force and torque.

2.5 Sizing of Actuators

At the end of this section, the size of actuators are estimated reflecting above discussions. Magnetic moment of $30,000[\mathrm{Am}^2]$ requires super-conductive magnet, and based on some discussions with super-conductive coil manufacturer, magnetic coil described in table 1 is practical enough and meets the requirements. The wire material is high-temperature superconducting one, thus the maximum temperature is 77 [K]. A cooling machine weight required to cool three coils is estimated to be 100 [kg].

Another component which should be discussed here is momentum wheels. As discussed, maximum disturbance torque caused by magnetic moment in earth magnetic field is about 0.9 [Nm], although accumulation as angular momentum could be negligible. On the other hand, the magnetic field of the other satellite causes small torque, however, it generates angular momentum such as 20 [Nms]. Momentum wheel of 10-15[kg] will have such capability of torque and angular momentum.

Table 1: Example spec. of required superconductive magnet.

Radius	Length	Wire Turns	Current	Weight
0.9 m	0.5 m	2381 T	15 A	40 kg

3 Relative Position Control System

3.1 Feedback Controller Design

Feedback controller design is briefly introduced in this subsection. The requirement for the controller is suppress the tidal disturbance force to achieve relative position accuracy of 2 [mm]. The constraint is that the control bandwidth must be lower enough than ω_c, since "average" magnetic force is used as the control input as expressed in Eq. 8. To meet these requirements and

the constraint, PID controller is designed using Coefficient Diagram Methods (CDM) [5], with following parameters,

$$K_I = \frac{12.5\mu_m}{\tau^3}, K_P = \frac{12.5\mu_m}{\tau^3}, K_D = \frac{5\mu_m}{\tau}, \tag{16}$$

where τ is so-called equivalent time constant and chosen to be 80[sec]. Fig. 4 shows the designed feedback controller performance with transfer function from disturbance to relative position. The frequency of two main disturbances, tidal disturbance and coil $2\omega_c$ disturbance, is also plotted.

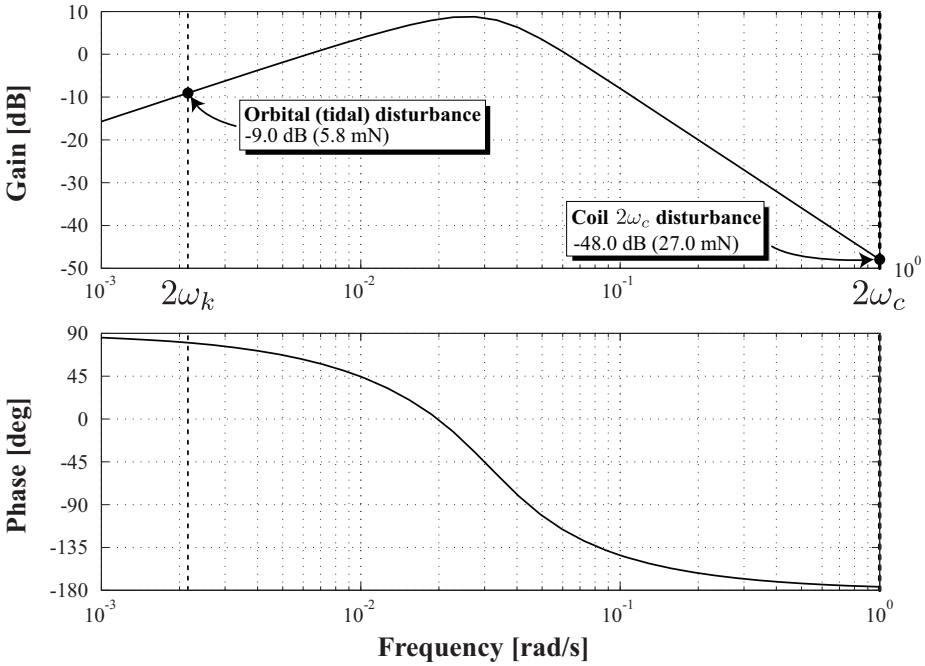

Fig. 4: Transfer function from disturbance to relative position.

3.2 Magnetic Force Regulator using Phase Difference between exciting currents

Basic idea to control the magnitude of magnetic force has already introduced in previous section, using Eq. 8 and Eq. 9. In this paper this concept is called "magnetic force regulator", and this section discusses the extension of Eq. 9 to three dimensional equation.

Equation 4 can be also expressed as

$$\boldsymbol{F} = \boldsymbol{D}\boldsymbol{B_C}, \tag{17}$$

where $\boldsymbol{D}$ is 3×3 symmetric matrix,

$$\boldsymbol{D} = \begin{bmatrix} \frac{\partial B_x}{\partial x} & \frac{\partial B_y}{\partial x} & \frac{\partial B_z}{\partial x} \\ \frac{\partial B_x}{\partial y} & \frac{\partial B_y}{\partial y} & \frac{\partial B_z}{\partial y} \\ \frac{\partial B_x}{\partial z} & \frac{\partial B_y}{\partial z} & \frac{\partial B_z}{\partial z} \end{bmatrix}. \tag{18}$$

The configuration of magnetic moment is depicted in Fig. 1, thus $\boldsymbol{M_T} = [0, 0, M_{Tz}]$. Using this $\boldsymbol{M_T}$, each element of this matrix can be developed,

$$\begin{aligned}
D_{11} &= D_{\text{mag}} \left\{ 2M_{Tx}x + (\boldsymbol{M_T} \cdot \boldsymbol{r}) - \frac{5\,(\boldsymbol{M_T} \cdot \boldsymbol{r})\,x^2}{\rho^2} \right\} \\
&= D_{\text{mag}} \left\{ M_{Tz}z - \frac{5M_{Tz}z}{\rho^2}x^2 \right\} \qquad (19) \\
D_{12} &= D_{\text{mag}} \left\{ M_{Ty}x + M_{Tx}y - \frac{5\,(\boldsymbol{M_T} \cdot \boldsymbol{r})\,yx}{\rho^2} \right\} \\
&= D_{\text{mag}} \left\{ -\frac{5M_{Tz}z}{\rho^2}xy \right\} \qquad (20) \\
D_{13} &= D_{\text{mag}} \left\{ M_{Tz}x + M_{Tx}z - \frac{5\,(\boldsymbol{M_T} \cdot \boldsymbol{r})\,zx}{\rho^2} \right\} \\
&= D_{\text{mag}} \left\{ -\frac{5M_{Tz}z}{\rho^2}zx \right\} \qquad (21) \\
&\cdots \\
D_{33} &= D_{\text{mag}} \left\{ 2M_{Tx}z + (\boldsymbol{M_T} \cdot \boldsymbol{r}) - \frac{5\,(\boldsymbol{M_T} \cdot \boldsymbol{r})\,z^2}{\rho^2} \right\} \\
&= D_{\text{mag}} \left\{ 3M_{Tz}z - \frac{5M_{Tz}z}{\rho^2}z^2 \right\}, \qquad (22)
\end{aligned}$$

where

$$D_{\text{mag}} = \frac{3\mu_0}{4\pi\rho^5}. \qquad (23)$$

To simplify Eq. 22, approximation around operational point is applied, $[x, y, z]^t = [\Delta x, \Delta y, z]^t$,

$$\begin{aligned}
D_{11} &= D_{\text{mag}} M_{Tz} z \left(1 - 5\frac{\Delta x^2}{z^2} \right) \\
D_{12} &= D_{\text{mag}} M_{Tz} z \left(-5\frac{\Delta y \Delta x}{z^2} \right) \\
D_{13} &= D_{\text{mag}} M_{Tz} z \left(-5\frac{\Delta x}{z} \right) \\
&\cdots \\
D_{33} &= -2D_{\text{mag}} M_{Tz} z, \qquad (24)
\end{aligned}$$

and if assume $\Delta x/z \ll 1$ and $\Delta y/z \ll 1$, the $\boldsymbol{D}$ comes to be diagonal matrix, with

$$\begin{aligned}
D_{11} &= D_{\text{mag}} M_{Tz} z, \qquad (25) \\
D_{22} &= D_{\text{mag}} M_{Tz} z, \qquad (26) \\
D_{33} &= -2D_{\text{mag}} M_{Tz} z. \qquad (27)
\end{aligned}$$

Therefore, each component of magnetic force, F_{Cx}, F_{Cy} and F_{Cz} can be independently controlled with M_{Cx}, M_{Cy} and M_{Cz}, respectively. These three components can be described easily with almost same equation, such as Eq. 8 or Eq. 9. Finally, phase difference which generates required force can be found to solve inversion problem of Eq. 9, using arc cosine or its linearly approximation [4].

4 Implementation and Experiments of Phase Difference Control

4.1 Proposed Circuit for Phase Difference and Amplitude Controller

This section discusses how to generate sinusoidal magnetic moment and how to control its phase. If current control technique is applied using power electronics devices, any required waveform of current can be generated, however, such approach is energy consuming. Therefore, it is proposed to use resonant circuit using superconductive coil and large capacitor, such as electric double layer capacitor. Then, how the phase should be controlled for such LC resonant circuit? The authors proposed to apply impulsive voltage input to change the phase of excitation current. Figure 5 shows the concept of the proposed method. As this figure shows, this method also has the capability to control the amplitude of the current. It is desirable capability, since there remains some small resistance in the whole circuit, even if superconductive coil is used.

The dynamics of the circuit depicted in Fig.6 can be analyzed as follows. With a state variable $\boldsymbol{x} = \begin{bmatrix} q & i_r \end{bmatrix}^T$,

$$\dot{\boldsymbol{x}} = \begin{cases} A_{off}\,\boldsymbol{x} & \ldots S{:}OFF \\ \\ A_{on}\,\boldsymbol{x} + B_{on}V_E & \ldots S{:}ON \end{cases} \tag{28}$$

$$A_{off} = \begin{bmatrix} 0 & -1 \\ \\ \dfrac{1}{LC} & -\dfrac{R_C}{L} \end{bmatrix}, \quad (\ R = R_E + R_C)$$

$$A_{on} = \begin{bmatrix} -\dfrac{1}{RC} & -\dfrac{R_E}{R} \\ \\ \dfrac{R_E}{RLC} & -\dfrac{R_E R_C}{RL} \end{bmatrix}, \quad B_{on} = \begin{bmatrix} \dfrac{1}{R} \\ \\ \dfrac{R_C}{RL} \end{bmatrix}.$$

where L, R_E, C, V_E are the value of inductance, resistance, capacitor and voltage source, respectively. q, i_r denotes the amount of capacitor charge and resonance current, respectively.

Using Eq. 28 and some approximations, the amount of phase shift $\Delta\phi$ and capacitor voltage change ΔV_c can be calculated when switch S is ON for Δt [sec] as follows,

$$\begin{aligned} \Delta v_{c0} &= \frac{1}{2R_E C}\left\{2V_E\cos\theta - v_{c0}\,(1+\cos 2\theta)\right\}\Delta t, \\ \Delta\phi &= -\frac{1}{2q_0 R_E}\left(2V_E\sin\theta - v_{c0}\sin 2\theta\right)\Delta t, \end{aligned} \tag{29}$$

where q_0, v_{c0} is the amplitude of capacitor charge and voltage. θ is the capacitor phase when switch S turns ON, and $\theta = 0$ means the capacitor voltage is equal to zero. Equation 29 indicates that both phase and amplitude can be controlled independently at $\theta = 2\pi n$ and $\theta = \pi/2 + 2\pi n$, respectively, where $n = 0, 1, 2 \ldots$.

4.2 Experimental Results of Phase Difference and amplitude Controll

Experiments using superconductive coil were carried out, to evaluate the proposed methods, to control the phase and amplitude of resonance current with impulsive voltage input. Fig. 8 is a

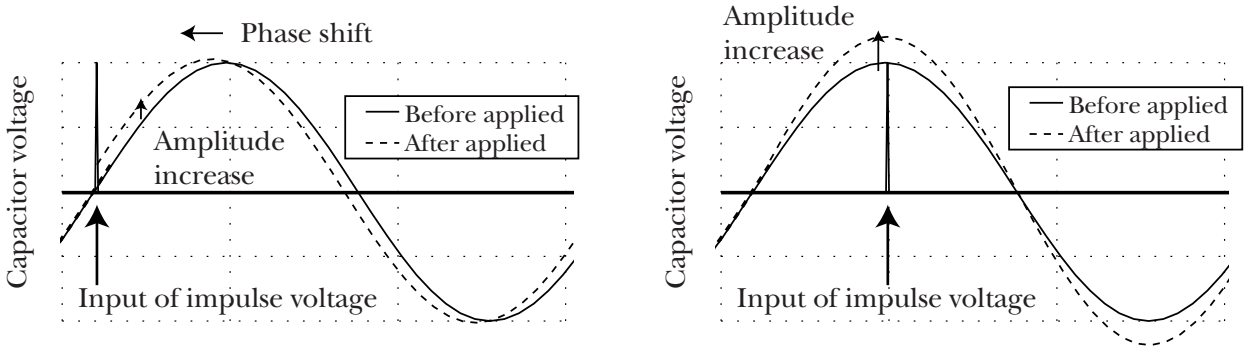

Fig. 5: The idea to shift the phase (left) and to change the amplitude (right) of the resonance current.

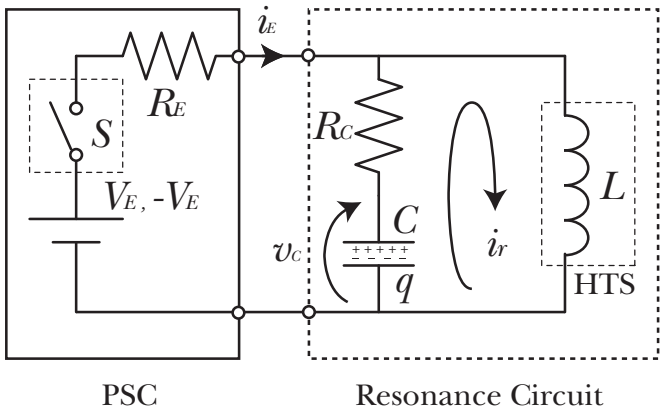

Fig. 6: Circuit structure to achieve phase-shifting and amplitude-changing of the resonant circuit.

photo of the experimental setup and Table 2 shows the specification of superconductive coil used in this experimental setup. In this setup, a current sensor measures the resonance current i_r, and it is transferred to the computer. The computer calculate the amount of Δt and waits the proper timing, the output a signal to turn on the switch S, which is implemented with FET device.

Figure 9 shows one example of experimental results. In this experiment, amplitude control was applied to sustain the resonance current against the resistance decay. Another experimental result is shown in Fig. 10, when dynamics phase control was applied. In this experiment, step reference of phase was input, and actual phase follows this reference with some time delay. Figure 11 plots the amount of phase shift and amplitude change, using both results of the actual experiments and the calculation of Eq. 29. These results indicate the effectiveness of proposed method for phase and amplitude control of coil exciting current.

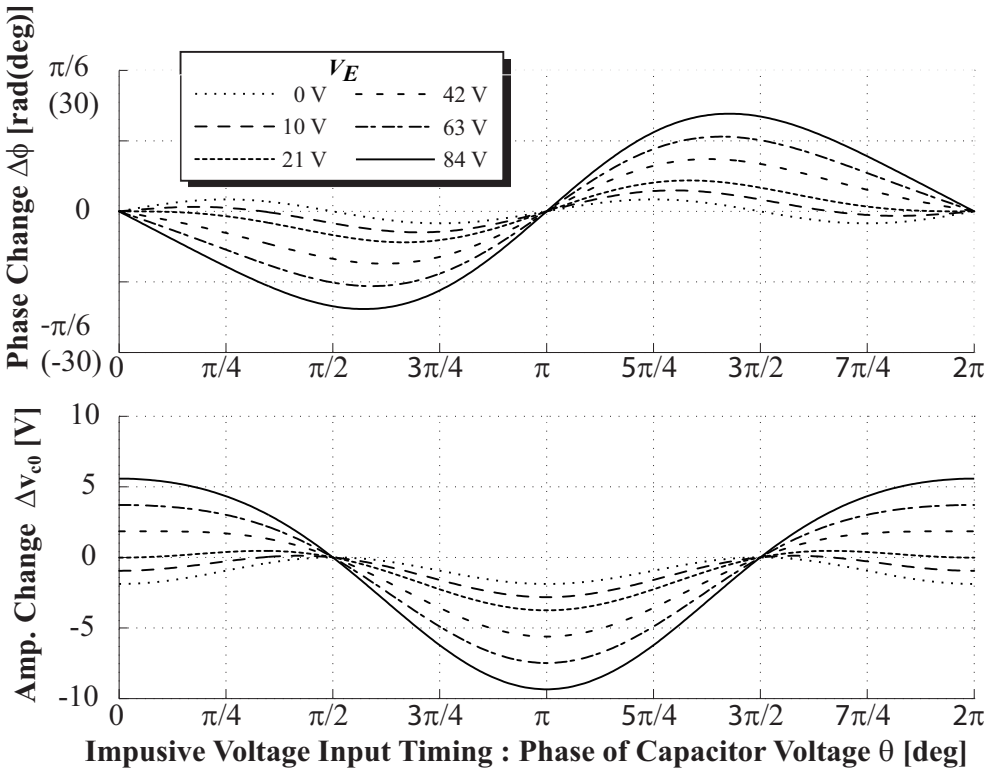

Fig. 7: Phase and amplitude change is plotted vs. voltage input timing θ, for various V_E.

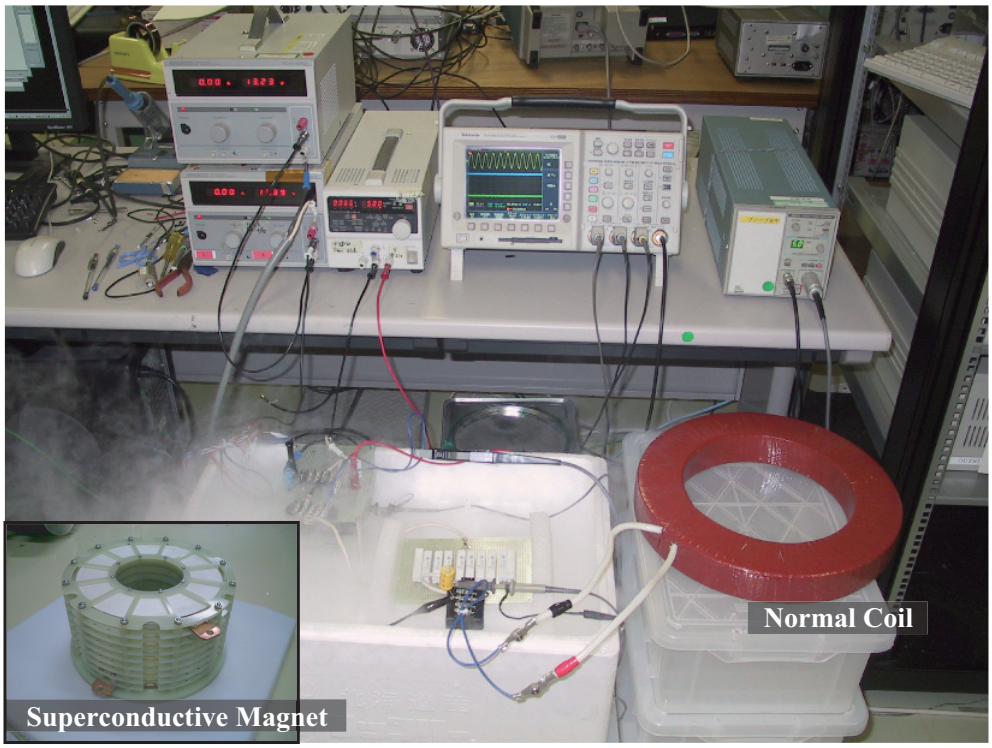

Fig. 8: Photo of experimental setup.

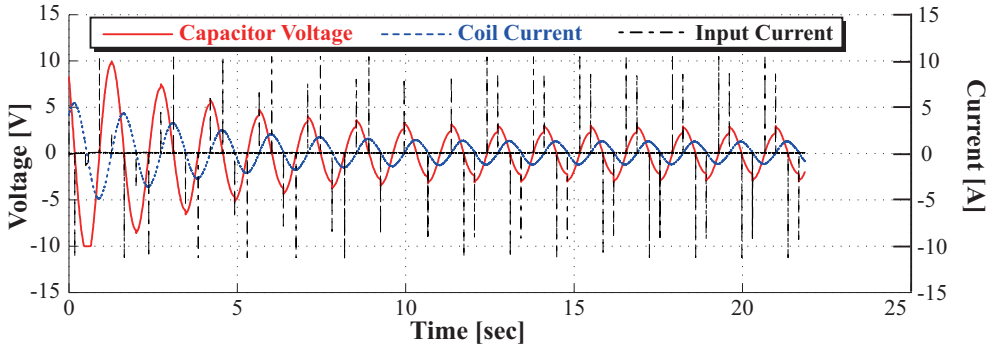

Fig. 9: Experimental result of amplitude control.

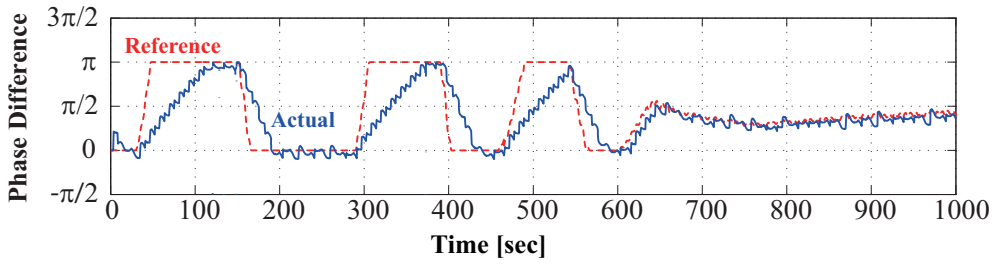

Fig. 10: Experimental result of phase difference control.

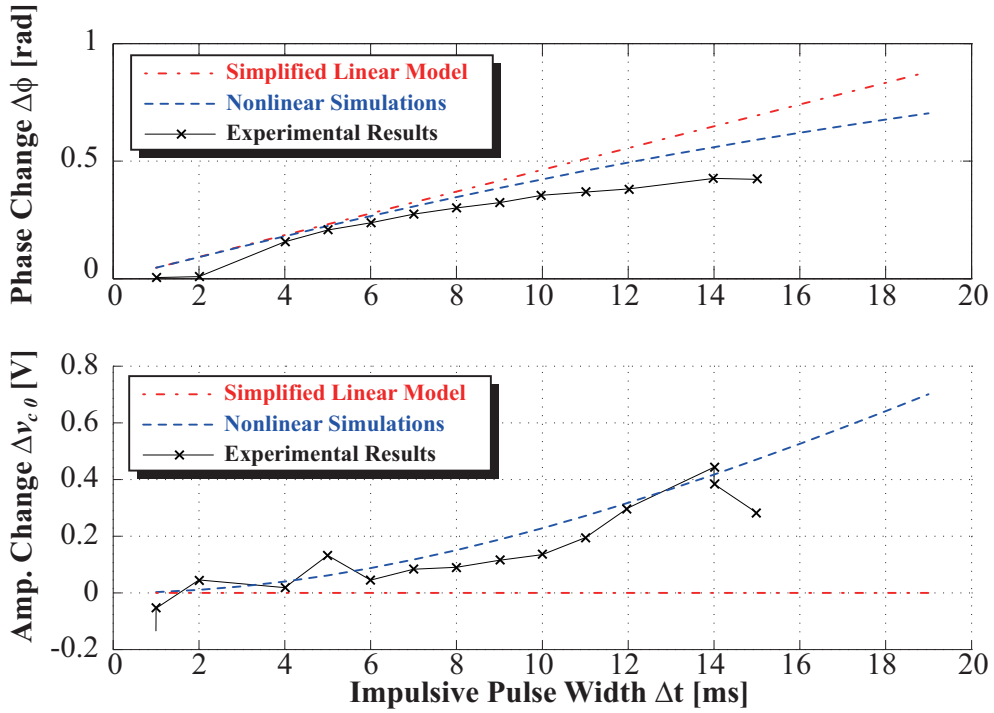

Fig. 11: Comparison of numerical model and experimental results for phase shift and amplitude change.

Table 2: Specification of superconductive coil for the experiments.

Coil Radius/Tickness/Length	3.7 / 3.9 / 9.5 [cm]
Coil Inductance	0.47 [H]
Wire Material	Bi2223

5 Evaluation with Hardware-in-the-loop Simulations

Finally, this section describes the demonstration of the proposed EMFF method using sinusoidal magnetic moment. As commonly known, the dynamics of spacecraft can be simulated with practical accuracy, and on the contrary, proposed phase control method should be evaluated more deliberately. From this perspective, hardware-in-the-loop simulations (HILS) were carried out. The setup for this HILS included actual hardware of superconductive magnet and drive circuit with proposed phase controller. Computer software measures the coil current by current sensors, then calculates the magnetic force and the satellites dynamics. The proposed relative position controller is also implemented in the same software, and output the reference of current phase difference. The hardware system described in the previous section controls the phase and amplitude of the actual resonance current, to follow this reference. Of course, the size of superconductive coil is smaller than the ones required for the satellites, thus the current value is multiplied by constant. Moreover, the resonance frequency is also different, 0.08 [Hz] and 0.7 [Hz] for actual satellite and HILS, respectively, thus the calculation in the HILS is for accelerated simulation. Figure 12 depicts the system configuration for this HILS. Pure computer simulations, which simulate also the coil current or phase controller, were also carried out for comparisons.

The control results of relative position is plotted in Fig. 13 for both HILS and pure computer simulation, and Fig. 14 is the enlarged view of the same results. In the initial condition, target satellite position is displaced from the reference position, by 0.2 [m] in $y-$ and $z-$ axis direction. This initial offset converged within 2000-3000[sec], and then the relative position error caused by tidal disturbance appears, e.g., on $x-$axis of Fig. 14. This residual error is about 1.0-2.0[mm], in consistency with estimation at the controller design. It indicates that the proposed system works properly. On the contrary, the z-axis response in HILS has position error of about 5.0 [mm]. The reason of this slightly large error is assumed to be the time delay of current phase control system, which was slightly worse than expectation.

Figure 15 is the time response of magnetic force on the chaser satellite. The results of HILS and numerical simulations almost meet with each other, indicating the validity of model or analysis about the phase control circuit.

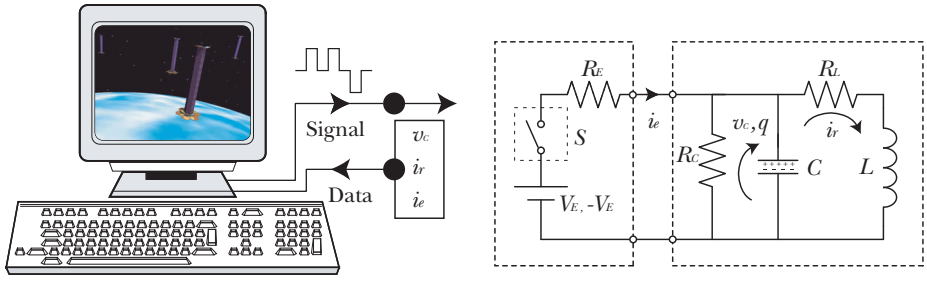

Fig. 12: HILS system using acutal superconductive coil and drive circuit.

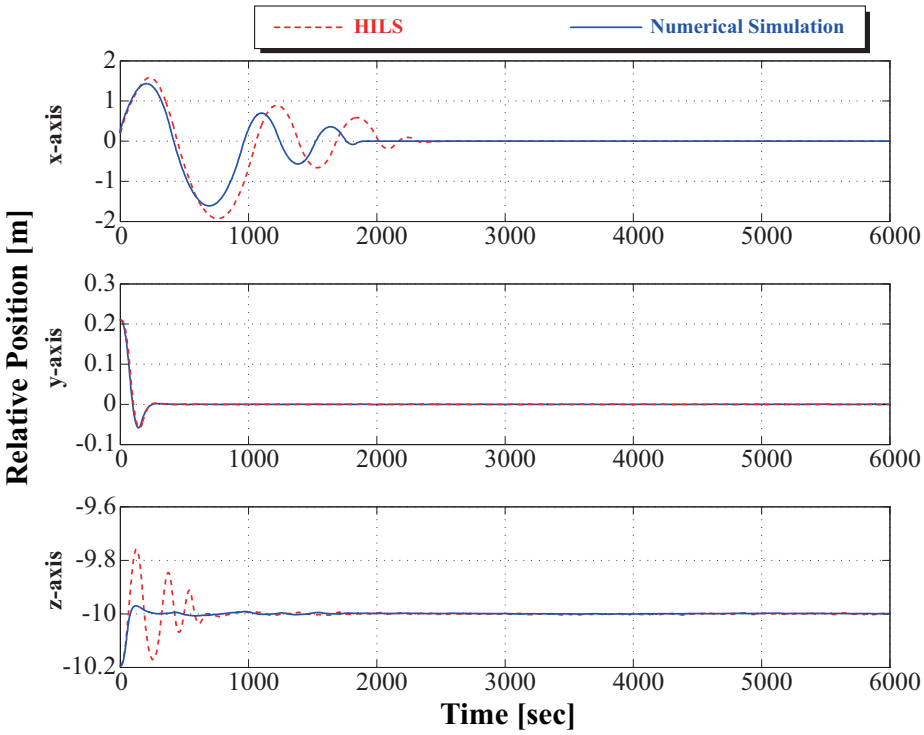

Fig. 13: Results of HILS and numerical simulation : relative position.

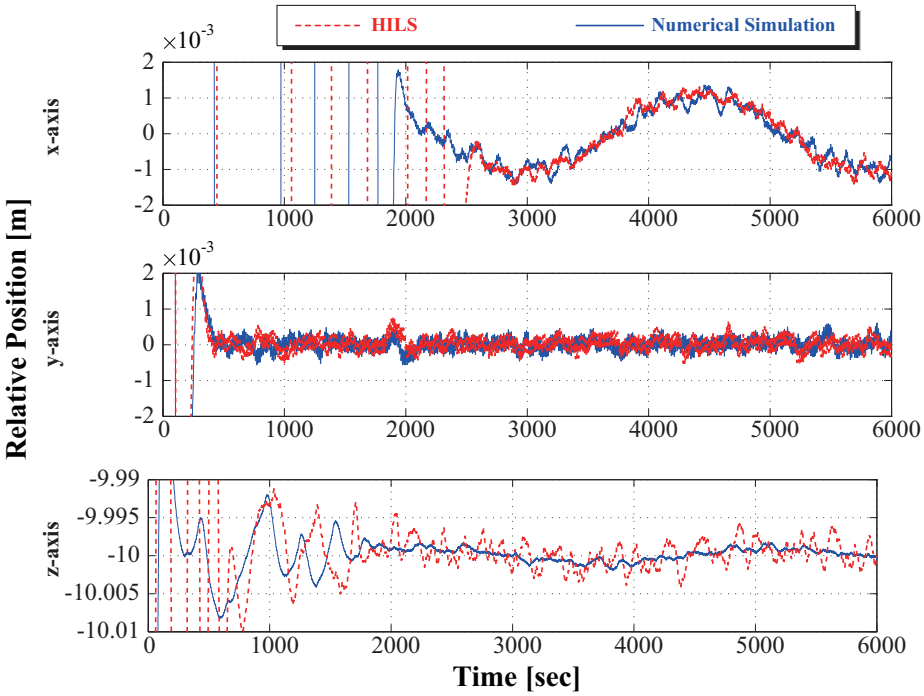

Fig. 14: Results of HILS and numerical simulation : relative position, closeup.

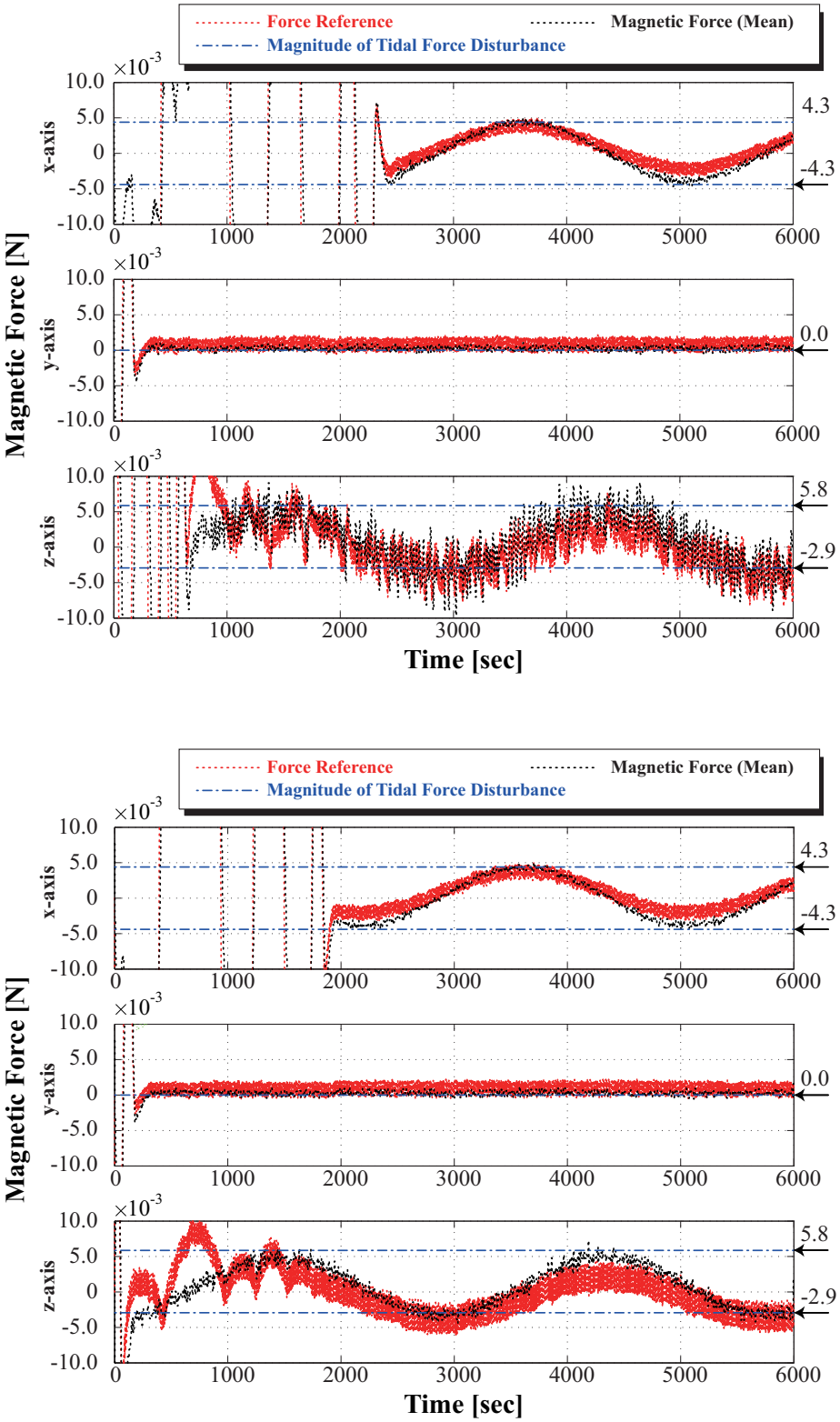

Fig. 15: Results of HILS (upper) and numerical simulation (lower) : magnetic force.

6 Conclusion

The electromagnetic formation flight (EMFF) using superconducting magnets was discussed, and it revealed that magnetic torque caused by earth magnetic field is serious problem to apply EMFF for LEO missions. Sinusoidal driving of magnetic moment and magnetic force control method using phase difference was proposed in this paper. Novel method to shift and control the resonance current using impulsive voltage input was also proposed, and it was evaluated with experimental results using actual superconducting coil. Then hardware in the loop simulation (HILS) was carried out, to demonstrate whole proposed method for relative position control. In this HILS, hardware of superconducting coil and phase control driving circuit was used with the software to calculate the satellites' dynamics. The results indicate the effectiveness of proposed methods for EMFF in LEO.

References

[1] Keiken Ninomiya, Tatsuaki Hashimoto, Shin-ichiro Sakai, Ken Maeda and Tetsuo Saitoh. Feasibility study of a formation flight control scheme using super-conductive magnet. In *Proc. of 11th Workshop on Astrodynamics and Flight Mechanics*, pp.175–181, Kanagawa, Japan, 2001.

[2] D.W. Miller, R. Sedwick, L. Elias and S. Schweighart. Electro-magnetic formation flight. In *Proc. of 26th annual AAS guidance and control conference*, Colorado, U.S., 2003.

[3] Tatsuaki Hashimoto, Shin-ichiro Sakai, Keiken Ninomiya, Ken Maeda and Tetsu Saitoh. Formation flight control using super-conducting magnet. In *Proc. of International Symposium Fomation Flying Missions & Technologies* (CD–ROM), Toulouse, France, 2002.

[4] Ryosuke Kaneda, Fumito Yazaki, Shin-ichiro Sakai, Tatsuaki Hashimoto and Hirobumi Saito. The relative position control in formation flying satellites using super-conducting magnets. In *Proc. of 2nd International Symposium on Formation Flying Missions & Technologies* (CD–ROM), No.79, Washington D.C, U.S., 2004.

[5] Syunji Manabe. The coefficient diagram method. In *Proc. of 14th IFAC Symposium on Automatic Control in Aerospace*, pp.199–210, Seoul, Korea, 1998.